QUASI-STATIC AND FATIGUE PERFORMANCE OF NON-TOUGHENED AND TOUGHENED ADHESIVES FOR WIND TURBINE BLADES

Dharun Vadugappatty Srinivasan[a], Anastasios P. Vassilopoulos[a]

a: Composite Construction Laboratory (CCLab), Ecole Polytechnique Fédérale de Lausanne
EPFL, Station 16, CH-1015 Lausanne, Switzerland.
dharun.srinivasan@epfl.ch

Abstract: *Epoxy adhesives used in wind turbine adhesive joints are non-toughened or moderately toughened to meet the loading requirements. Adhesive toughening is not generally cost-effective and such newly modified adhesives need further certification to be used in wind turbine blades. Alternatively, hybrid adhesives with tailored mechanical properties can be attained using commercially available adhesives. In this study, glass fiber and rubber particle modified adhesives are used to fabricate pristine and a combination of hybrid adhesives through two different manufacturing techniques. The glass transition temperature and quasi-static mechanical properties are insensitive to the manufacturing defects. Tensile modulus, tensile strength, shear modulus, shear strength, and fracture toughness are decreased by toughening. Further two different ASTM D638-14 Type I sample and Type II samples are considered to determine the influence of size effect on the tensile fatigue performance.*

Keywords: Adhesives; toughening; fatigue; size effect; failure analysis

1. Introduction

Adhesive bonding is widely used in large-scale structures such as aircraft, wind turbine blades and automobiles as it offers nearly uniform stress distribution and less assembly weight as compared with mechanical fasteners. In these applications, non-toughened and toughened epoxy adhesives are typically found due to their inherent mechanical and chemical properties. The non-toughened epoxy adhesive has higher mechanical stiffness, strength and cost-effectiveness as compared with toughened adhesives. But non-toughened adhesives possess poor strain to failure, crack resistance and impact resistance that can be improved by adhesive toughening However, toughening introduces flexible materials and chains inside the rigid epoxies, and it may reduce other mechanical properties such as tensile modulus and tensile strength as well as the temperature-related performance [1]. Implementing the high-cost toughening strategies in these large bond volume applications is not practically feasible. Hence, hybrid adhesives with desirable mechanical properties should be developed using commercially available adhesives. So, further certification of these adhesives is not required and can be readily used by the blade manufacturers. Epoxy base and hardener in paste forms are highly viscous and generally mixed by a mechanical mixer before applying to the bonding surface. This method is practiced by blade manufacturers to avoid air voids and control the bond quality. In other scenarios such as adhesively bonded local repair process and academic research, manual mixing is commonly followed. In the manual mixing process, the adhesive and hardener can be poorly mixed, and voids can be introduced while mixing or adhesive deposition process Most of these studies in the literature were focused only on the toughening effect on the DMA, tensile and fracture properties but not on the shear strength. The discussed toughening methods could not

be readily used by wind turbine blade manufacturers. Hence new hybridization strategies reducing the certification process, time and cost need to be developed.

The joints are also subjected to various loadings including static, fatigue [2], impact and environment during the service. Designing the adhesive joints for the above-combined loading conditions is challenging, as the joint performance depends on different parameters such as the joint geometry [3], adherend material, adhesive constituent properties, surface preparation, curing conditions [4–7] and post-curing [8] conditions. Savvilotidou et al. [9,10] studied the effect of moisture on the physical, quasi-static tensile and tensile fatigue life of the epoxy adhesives used in bridges and it can withstand the fatigue stresses higher than 25 % of their static tensile strength for more than 2 million cycles. There is only limited work carried out on the fatigue performance of the structural epoxy adhesives. The effect of hybrid toughening under the fatigue loading needs to be investigated as it would aid in tailoring the adhesive properties according to the load levels and fatigue life. The tensile fatigue samples are tested as recommended by ASTM D638-14 Type I sample and Type II samples geometric configuration and they are suggested by ASTM D7791-17, a standard test method for measuring fatigue properties of plastics. These samples have a width of 13 mm and 6 mm, respectively which may affect the fatigue life. To the best of the author's knowledge, there was no study exploring the size effect of these testing geometries on the fatigue performance of the epoxy adhesives.

In this work, glass fiber and rubber particle modified adhesives were used to fabricate pristine and hybrid adhesives through two different manufacturing techniques and hybridization strategies. The manufacturing and hybridization effects on the material properties were evaluated by dynamic mechanical analysis (DMA), quasi-static tensile, V-notch shear and single-edge-notch bending (SENB) testing. The hybridization effects on the fatigue performance were evaluated through S-N diagrams. Further, ASTM D638-14 Type I sample and Type II samples were tested at different load levels to determine the influence of size-effect.

2. Materials and manufacturing

Two different epoxy-based paste adhesives SPABOND™ (SP) 820HTA and SPABOND™ 840HTA provided by Gurit (UK) Ltd were used to fabricate the pristine (BBM1, TTM1, BBM2 and TTM2) and hybrid adhesives (BTM1, TBM1, BTM2 and TBM2). SP 820HTA is a glass fiber-filled, non-toughened adhesive (BB) [13] whereas SP 840HTA is toughened with core-shell rubber particles (TT) [14]. Two different manufacturing methods M1 and M2 are also considered in this study. In the first manufacturing method (M1), the epoxy base and hardener were mixed thoroughly using a mechanical mixer at a weight ratio of 100:33, as practiced by the wind turbine industries. M1 panels were fabricated and provided by Gurit (UK) Ltd. In the manual mixing method (M2), wooden spatulas were used to mix the adhesive materials for 5 to 7 minutes and degassed at 0.95 bar of vacuum for 5 to 10 minutes. After degassing, the adhesive was spread inside the aluminium mold cavity (4 mm) layer by layer. The mixed adhesive system was cured at the ambient temperature for 120 minutes which includes the adhesive mixing and degassing processes, to mimic the time taken by the blade manufacturers for applying adhesive on the long wind turbine blades. Lately, the adhesive was heated to 70°C at a rate of 2 °C⁄min and cured for 120 minutes.

In this study, two different hybridization strategies are considered to develop the new hybrid adhesives. As illustrated in Figure 1a, the hardener of non-toughened and toughened adhesives was swapped in the first strategy. BTM1 hybrid adhesive was prepared by mixing SP 820HTA

base and SP 840HTA hardener and vice-versa for TBM1 hybrid adhesive. The above strategy is cost-effective, as any one of the hardener and base materials was used for tailoring the material properties. The second hybridization strategy is mixing the non-toughened adhesive (base with hardener) and toughened adhesive (base with hardener) at certain weight proportions. Figure 1b shows that the hybrid adhesives, BTM2 and TBM2 were prepared by mixing the toughened adhesive with non-toughened adhesive at 25 wt% and 50 wt%, respectively. Samples fabricated through M2 technique only were used in fatigue testing.

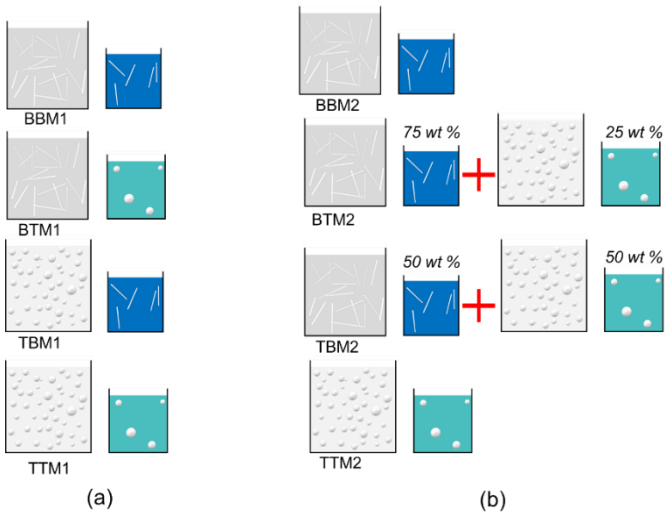

Figure 1. Schematic diagram of adhesive material composition: (a) M1, machine mixing method and (b) M2, manual mixing method.

3. Test methods

3.1 Dynamical mechanical analysis

DMA samples were tested under single cantilever mode using TA® Q800 series machine as stipulated by ASTM D7028-07 (2015). Liquid nitrogen was supplied to the test machine for capturing the DMA properties at a lower temperature (-50℃). The sample was aligned well into the fixture using a torque of 1.47 Nm and heated from -50℃ to 150℃ at a rate of 5 °C⁄min. The oscillating frequency was set to 1 Hz with an amplitude of 20 µm.

3.2 Quasi-static tensile and V-notch shear testing

Uniaxial tensile test was conducted using MTS® 810 Landmark servo-hydraulic machine with a calibrated load cell capacity of 5 kN and applied force accuracy of ±5%. The ASTM D638-14 Type I sample was tested under displacement control, at a crosshead rate of 1 mm/min. All the tests were performed at the ambient temperature of 22 ± 3°C and relative humidity of 40 ± 10%.

V-notch shear sample was prepared as recommended in ASTM D5379-19. Walter + bai (w + b) test machine equipped with a load cell capacity of 50 kN and Iosipescu shear fixture was used to perform the shear tests. The top punch was displacement-controlled at a rate of 1 mm/min.

3.3 Single-edge-notch bending (SENB)

MTS® Acumen equipped with a 3 kN load cell and a three-point bending fixture was used in the plane strain fracture toughness testing. The sample was adjusted in the fixture such that the

initial notch and the contact point of the top roller were on the same loading axis. The top roller was loaded at a displacement rate of 0.25 mm/min to have a stable fracture. During the testing, 2D DIC images were captured from which the mid-span deflection was calculated. In order to have an effective K_{IC}, the load P_Q was selected as mentioned in ASTM D5045-14.

3.4 Tensile-Tensile fatigue testing

The fatigue experiments were conducted using the same MTS® machine and the samples were force-controlled with a stress ratio R of $\sigma_{min}/\sigma_{max} = 0.1$. The selected R ratio prevents compressive stress in the sample and buckling instability hence, the test results can be compared with the literature values. True sinusoidal loads were applied with a frequency of 10 Hz.

4. Results and discussion

4.1 Hybridization and manufacturing effect on DMA properties

Glass transition temperature, peak $tan\,\delta$ and E' at 25℃ of the M1 adhesives are given in Table 1. Within the experimental scatter, T_g of all the adhesives lies between 71.4℃ to 76.9℃ and there was no significant effect of the first hybridization strategy on T_g. The non-toughened adhesive (BBM1) has higher E' and lower $tan\,\delta$ than the hybrid (BTM1 and TBM1) and toughened (TTM1) adhesives. Due to higher toughening content, the storage modulus of TBM1 adhesive was 23% lesser than BTM1 adhesive. T_g was not significantly affected by the second hybridization strategy implicating that these non-toughened and toughened adhesives can be mixed or cured together for developing tailored adhesive joints.

Table 1: DMA properties of M1 and M2 adhesives.

Sample	T_g (℃)	Peak $tan\,\delta$ (-)	E' at 25℃ (GPa)
BBM1	73.4±0.5	0.623±0.003	3.18±0.17
BTM1	75.4±1.8	0.614±0.014	2.91±0.17
TBM1	74.5±1.6	0.663±0.009	2.36±0.05
TTM1	71.4±0.7	0.723±0.007	2.22±0.15
BBM2	72.6±0.8	0.613±0.005	2.98±0.10
BTM2	76.9±0.4	0.620±0.007	2.63±0.03
TBM2	76.1±2.9	0.648±0.008	2.68±0.13
TTM2	72.8±1.7	0.748±0.003	2.06±0.20

4.2 Hybridization and manufacturing effect on tensile properties

The measured tensile properties of the adhesives are provided in Table 2. The tensile modulus of BBM1 adhesive is 10.4%, 32.7% and 41.6% higher than BTM1, TBM1 and TTM1 adhesives, respectively. The yield stress of BTM1 adhesive was 6.2% lower than BBM1 adhesive. While considering the first hybridization strategy, TBM1 adhesive showed a distinct elastic-plastic tensile behaviour than BTM1 adhesive, hence it can be used in practical applications. Similarly, the average tensile modulus of BBM2 adhesive was 11.4%, 28% and 50% higher than BTM2,

TBM2 and TTM2 adhesives, respectively. An increase in M2 adhesive toughening also caused increase in the scattering of the failure strain.

Table 2. Uniaxial tensile properties of the adhesives.

Sample	Tensile modulus (E)	0.2% offset Yield stress (σ_y)	Tensile toughness (U_T)	Tensile strength (σ_u)	Failure strain (ε_f)
	GPa	MPa	kJ/m^3	MPa	mm/mm
BBM1	5.1±0.08	51.38±1.89	0.68±0.14	60.16±2.65	0.0179±0.0024
BTM1	4.57±0.22	54.78±1.12	0.69±0.12	61.17±2.18	0.0184±0.0017
TBM1	3.43±0.07	42.20±2.27	1.26±0.17	52.56±0.64	0.0329±0.0027
TTM1	2.98±0.14	38.69±0.89	1.38±0.11	45.36±0.15	0.0391±0.0023
BBM2	5.59±0.39	61.47±1.75	0.71±0.03	69.01±0.51	0.0170±0.0007
BTM2	4.95±0.32	55.65±1.95	0.84±0.10	65.01±2.23	0.0201±0.0010
TBM2	4.02±0.06	47.21±0.39	0.96±0.11	55.98±0.87	0.0248±0.0020
TTM2	2.81±0.16	37.86±0.55	1.45±0.20	44.47±1.26	0.0417±0.0054

4.3 Hybridization and manufacturing effect on shear properties

The shear modulus, strength and failure strain of the adhesives are given in *Table 3*. The shear modulus and strength of the adhesives vary between 0.73 GPa to 2.12 GPa and 36.91 MPa to 51.65 MPa. Based on the required joint stiffness and shear strength in real-time applications, any one of these adhesives can be selected.

Table 3. Shear properties of the adhesives.

Sample	Shear modulus (G)	Shear strength (τ_u)	Failure shear strain (γ_f)
	GPa	MPa	mm/mm
BBM1	2.12±0.19	51.02±1.79	0.0601±0.0102
BTM1	1.13±0.03	51.50±1.14	0.0695±0.0019
TBM1	0.80±0.04	41.19±0.20	0.1316±0.01
TTM1	0.73±0.06	36.91±1.11	0.1574±0.0431
BBM2	1.90±0.50	51.65±1.70	0.0539±0.0035
BTM2	1.63±0.06	46.54±0.34	0.0399±0.0042
TBM2	1.57±0.05	43.03±0.29	0.0435±0.0013
TTM2	0.91±0.09	38.10±1.31	0.12±0.03

4.4 Hybridization and manufacturing effect on fracture toughness

K_{IC} of the BBM1, BTM1, TBM1 and TTM1 adhesives are 1.84 ± 0.17 $MPa\sqrt{m}$, 2.12 ± 0.18 $MPa\sqrt{m}$, 2.17 ± 0.05 $MPa\sqrt{m}$ and 1.63 ± 0.05 $MPa\sqrt{m}$, respectively. Within the experimental

scatter, the K_{IC} of BBM2 (2.64 ± 0.12 $MPa\sqrt{m}$), BTM2 (2.39 ± 0.17 $MPa\sqrt{m}$) and TBM2 (2.43 ± 0.27 $MPa\sqrt{m}$) adhesives were found to be similar. K_{IC} of TTM2 adhesive is 23.86% lower than the BBM2 adhesive. The fracture toughness of BBM2 and TTM2 adhesives are comparable to the technical data sheet values [13,14]. The fracture behaviour of TTM1 and TTM2 were similar however BBM1 was failed at a lower force than BBM2 adhesive. BBM1 fracture surface shows more fiber debonding than fiber breakages that can be corelated to the orientation of glass fibers at the middle section. Therefore, tensile and fracture behaviour of glass fiber modified adhesives are influenced by the fiber orientation compared with shear.

4.5 Size effect and hybridization effect on fatigue life

The S-N plots of the adhesives and their corresponding fit based on Basquin's fatigue law using CCLab fatigue software are shown in Figure 2. As illustrated in Figure 2a and 2b, the slope of type II samples of BBM2 and BTM2 adhesives are 13.45% and 6.82% lesser than that of type I samples, respectively. The higher width (13 mm) samples could have more defects as compared with the lower width, type II samples. Comparing all the adhesives, the slop was not influenced by the adhesive toughening. All the samples manifested brittle fracture at the end of the life, as there was no increase in the displacement or strain during the final failure stage. The stiffness degradation of the adhesives was higher at the high load level than at the lower stress levels.

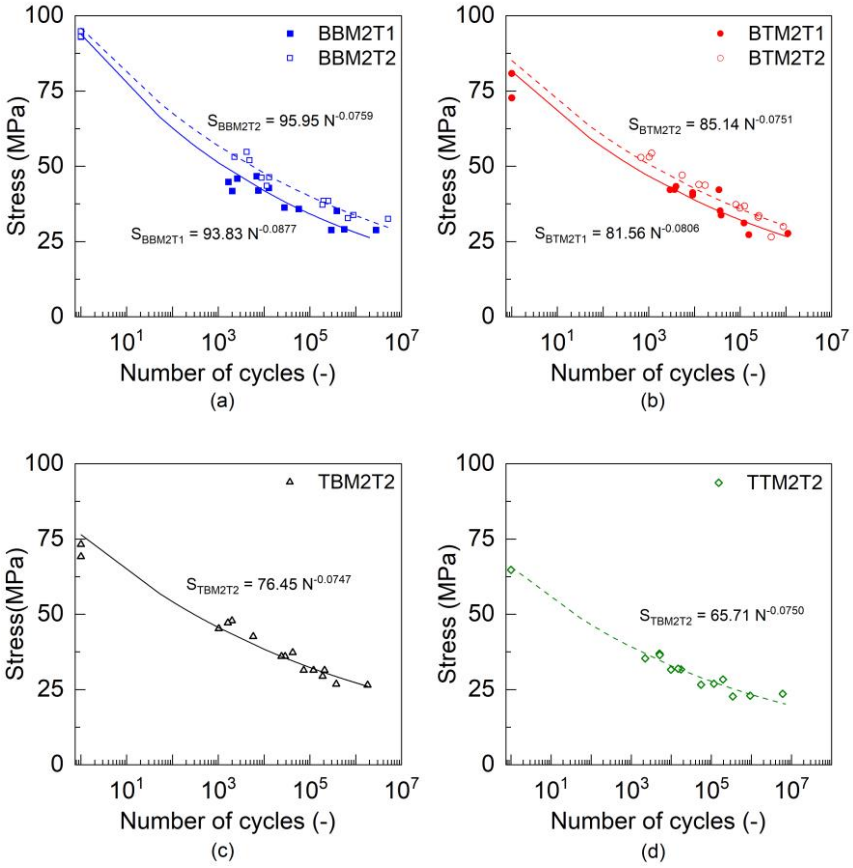

Figure 2. S-N curves of the adhesives: (a) BBM2T1 & BBM2T2, (b) BTM2T1 & BTM2T2, (c)TBM2T2 and (d)TTM2T2.

5. Conclusions

From the experimental study, the following conclusions are made: (a) The tensile modulus, tensile strength, shear modulus, shear strength and critical plane strain fracture toughness were decreased with an increase in toughening. However, the failure strain and tensile toughness were increased with toughening; (b) The tensile strength of the adhesives was decreased more than the shear strength with respect to toughening; (c) Among the developed hybrid adhesives, BTM1 adhesive showed better material properties and this hybridization strategy is recommended in practical applications and (d) Adhesive toughening has a less effect on the slope of S-N curve. On the contrary, the size effect shows a change in the slope of S-N curves.

Acknowledgements

The authors wish to acknowledge the support and funding of this research by the Swiss National Science Foundation (Grant No. IZCOZ0_189905) under the project, Bonded composite primary structures in engineering applications (BONDS). The authors also acknowledge the experimental assistance provided by the technical team of the structural engineering experimental platform (GIC-ENAC) at the Ecole Polytechnique Fédérale de Lausanne (EPFL), Switzerland. The authors also thank Gurit UK Ltd for providing adhesive materials and for many helpful discussions. The authors thank Marc Edmond for his kind help in CT scan image analysis. This article/publication is based upon work from COST Action CA18120 (CERTBOND - https://certbond.eu/), supported by COST (European Cooperation in Science and Technology).

6. References

1. Kinloch AJ, Lee SH, Taylor AC. Improving the fracture toughness and the cyclic-fatigue resistance of epoxy-polymer blends. Polymer (Guildf). 2014; 55(24):6325–34.
2. Rosemeier M, Krimmer A, Bardenhagen A, Antoniou A. Tunneling crack initiation in trailing-edge bond lines of wind-turbine blades. AIAA Journal. 2019; 57(12):5462–74.
3. Tang JH, Sridhar I, Srikanth N. Static and fatigue failure analysis of adhesively bonded thick composite single lap joints. Composites Science and Technology. 2013; 86:18–25.
4. Czaderski C, Martinelli E, Michels J, Motavalli M. Effect of curing conditions on strength development in an epoxy resin for structural strengthening. Composites Part B: Engineering. 2012; 43(2):398–410.
5. Michels J, Sena Cruz J, Christen R, Czaderski C, Motavalli M. Mechanical performance of cold-curing epoxy adhesives after different mixing and curing procedures. Composites Part B: Engineering. 2016; 98:434–43.
6. Carbas RJC, Marques EAS, da Silva LFM, Lopes AM. Effect of Cure Temperature on the Glass Transition Temperature and Mechanical Properties of Epoxy Adhesives. https://doi.org/101080/002184642013779559. 2013; 90(1):104–19.
7. I. M. Foletti A, Sena Cruz J, Vassilopoulos AP. Fabrication and curing conditions effects on the fatigue behavior of a structural adhesive. International Journal of Fatigue. 2020; 139:105743.

8. Carbas RJC, da Silva LFM, Marques EAS, Lopes AM. Effect of post-cure on the glass transition temperature and mechanical properties of epoxy adhesives. http://dx.doi.org/101080/016942432013790294. 2013; 27(23):2542–57.
9. Savvilotidou M, Keller T, Vassilopoulos AP. Fatigue performance of a cold-curing structural epoxy adhesive subjected to moist environments. International Journal of Fatigue. 2017; 103:405–14.
10. Savvilotidou M, Vassilopoulos AP, Frigione M, Keller T. Effects of aging in dry environment on physical and mechanical properties of a cold-curing structural epoxy adhesive for bridge construction. Construction and Building Materials. 2017; 140:552–61.
11. SPABOND 820HTA™ Fast curing structural epoxy adhesive. Full general datasheet [Internet]. Available from: www.gurit.com.
12. SPABOND™ 840HTA fast curing structural epoxy adhesive. Full general datasheet [Internet]. Available from: www.gurit.com.

